On-Line Monitoring of Apoptosis in Insulin-Secreting Cells

Martin Köhler,[1] Sergei V. Zaitsev,[1,2] Irina I. Zaitseva,[1,2] Barbara Leibiger,[1] Ingo B. Leibiger,[1] Mikael Turunen,[1] Iouri L. Kapelioukh,[1,2] Linda Bakkman,[1] Ioulia B. Appelskog,[1] Jacques Boutet de Monvel,[3,4] Gabriela Imreh,[1] and Per-Olof Berggren[1]

Apoptosis was monitored in intact insulin-producing cells both with microfluorometry and with two-photon laser scanning microscopy (TPLSM), using a fluorescent protein based on fluorescence resonance energy transfer (FRET). TPLSM offers three-dimensional spatial information that can be obtained relatively deep in tissues. This provides a potential for future in vivo studies of apoptosis. The cells expressed a fluorescent protein (C-DEVD-Y) consisting of two fluorophores, enhanced cyan fluorescent protein (ECFP) and enhanced yellow fluorescent protein (EYFP), linked by the amino acid sequence DEVD selectively cleaved by caspase-3–like proteases. FRET between ECFP and EYFP in C-DEVD-Y could therefore be monitored on-line as a sensor of caspase-3 activation. The relevance of using caspase-3 activation to indicate β-cell apoptosis was demonstrated by inhibiting caspase-3–like proteases with Z-DEVD-fmk and thereby showing that caspase-3 activation was needed for high-glucose– and cytokine-induced apoptosis in the β-cell and for staurosporine-induced apoptosis in RINm5F cells. In intact RINm5F cells expressing C-DEVD-Y and in MIN6 cells expressing the variant C-DEVD-Y2, FRET was lost at 155 ± 23 min (n = 9) and 257 ± 59 min (n = 4; mean ± SE) after activation of apoptosis with staurosporine (6 μmol/l), showing that this method worked in insulin-producing cells. *Diabetes* 52:2943–2950, 2003

Apoptosis plays an important role in the development of diabetes (1). The main cause of type 1 diabetes is the loss of β-cell mass as a result of inflammation in pancreatic islets and effects of toxic agents on pancreatic β-cells resulting in apoptosis (2). Cytokines, especially interleukin-1β (IL-1β), interferon-γ (INF-γ), and tumor necrosis factor-α (TNF-α), play an important role in apoptotic β-cell destruction (2). We have previously shown the existence of a factor in the serum of newly diagnosed type 1 diabetic patients causing apoptosis of pancreatic β-cells (3). Current studies demonstrate that apoptosis of pancreatic β-cells takes place also in type 2 diabetes (4,5), although the mechanism behind this process is not understood. We have demonstrated that glucose, a principal regulator of pancreatic β-cell function, at high concentration causes apoptotic β-cell death in pancreatic islets from rats and mice (6). Moreover, in the same study, we showed that sulfonylurea compounds, currently used drugs for the treatment of type 2 diabetes, trigger apoptosis of pancreatic β-cells. All of this information points to the importance of studies of pancreatic β-cell apoptosis, both for understanding the mechanisms that cause diabetes and for the development of treatments of the disease. Whereas a number of procedures for evaluating β-cell apoptosis have been described, there is currently no available noninvasive method allowing on-line monitoring of apoptosis in living β-cells in vitro or in vivo. We now describe a noninvasive method that can be used for on-line detection of apoptosis in single β-cells by two-photon laser scanning microscopy (TPLSM), using fluorescence resonance energy transfer (FRET). Here we illustrate the method by on-line studies of apoptosis in the β-cell lines RINm5F and MIN6. The technique is based on monitoring of apoptotic stimuli-induced activation of caspase-3–like proteases. The activity of caspase-3–like proteases is monitored through a fluorescent probe based on FRET between enhanced cyan fluorescent protein (ECFP) and enhanced yellow fluorescent protein (EYFP) in an expressed hybrid protein consisting of ECFP and EYFP linked by a spacer containing the amino acid sequence DEVD, which is specific for substrates of these enzymes (7). Both ECFP and EYFP are variants of green fluorescent protein, which is highly resistant to various proteases (8). On the contrary, the DEVD sequence is cleaved by activated caspase-3–like proteases. This cleavage leads to spatial separation of ECFP and EYFP and results in a loss of measurable FRET. Fluorescence from ECFP and EYFP can be monitored simultaneously by fluorometric techniques including TPLSM, providing a ratiometric measure of apoptosis. Use of TPLSM for these measurements will minimize cell damage and permit studies of cells that are located deeper into tissues compared with confocal

From the [1]Rolf Luft Center for Diabetes Research, Department of Molecular Medicine, Karolinska Institutet, Karolinska Hospital, Stockholm, Sweden; the [2]Belozersky Institute of Physico-Chemical Biology and Chemical School, Lomonosov Moscow State University, Moscow, Russia; the [3]Center for Hearing and Communication Research and Department of Clinical Neuroscience, Karolinska Institutet, Stockholm, Sweden; and the [4]Department of Otolaryngology, Karolinska Hospital, Stockholm, Sweden.

Address correspondence and reprint requests to Martin Köhler, the Rolf Luft Center for Diabetes Research, Department of Molecular Medicine, Karolinska Institutet, Karolinska Hospital, SE-171 76 Stockholm, Sweden. E-mail: martin.kohler@molmed.ki.se.

Received for publication 7 May 2003 and accepted in revised form 29 August 2003.

M.K. and S.V.Z. contributed equally to this study.

DIC, differential interference contrast; DWT, discrete wavelet transform; ECFP, enhanced cyan fluorescent protein; EYFP, enhanced yellow fluorescent protein; FRET, fluorescence resonance energy transfer; IL-1β, interleukin-1β; INF-γ, interferon-γ; TNF-α, tumour necrosis factor-α; TPLSM, two-photon laser scanning microscopy; TUNEL, transferase-mediated dUTP nick-end labeling.

laser-scanning microscopy (9,10). A part of this study was presented in abstract form (11).

RESEARCH DESIGN AND METHODS

Materials. RPMI 1640 medium, FCS, Lipofectamine 2000, and geneticin G-418 were obtained from Gibco BRL (Life Technologies, Gaithersburg, MD). The fluorescent dye Hoechst 33342 was from Molecular Probes (Eugene, OR). Recombinant human IL-1β, Z-DEVD-fmk, RNAse, and the kit for transferase-mediated dUTP nick-end labeling (TUNEL) reaction were purchased from Boehringer Mannheim (F. Hoffmann-La Roche, Basel, Switzerland). All other reagents were of analytical grade and obtained from Sigma (St. Louis, MO).

Isolation of pancreatic β-cells. Ten- to 12-month-old obese nondiabetic (*ob/ob*) mice, obtained from a local colony, were used. Pancreatic islets from *ob/ob* mice contain >90% β-cells (12,13). Islets were isolated by collagenase digestion and dispersed into small β-cell clusters in Ca^{2+}- and Mg^{2+}-deficient medium, as previously described (14). Cells were cultured on glass coverslips in plastic Petri dishes for 40 h in RPMI 1640 medium containing 10% (vol/vol) FCS, 100 IU/ml penicillin, and 100 μg/ml streptomycin in the presence of 11 or 17 mmol/l glucose or 11 mmol/l glucose and 2 ng/ml IL-1β and in the presence or in the absence of 50 μmol/l Z-DEVD-fmk.

TUNEL labeling of pancreatic β-cells and double staining for confocal microscopy. The TUNEL technique was used to detect DNA strand breaks in situ as previously described (6). Cells that were double stained with fluorescein isothiocyanate and propidium iodide were fixed on glass slides with 50% glycerol in PBS. Fluorescence was monitored with a Leica TCS-NT laser scanning confocal microscope (Leica Microsystems Heidelberg, Mannheim, Germany), with excitation from the 488-nm line of a Argon/Krypton laser. Fluorescence emission was detected with a bandpass filter (from Chroma Technology, Brattleboro, VT) centered at 530 nm for fluorescein isothiocyanate and above 590 nm for propidium iodide. Several confocal images were used for counting the number of apoptotic cells detected by the TUNEL method. In each condition, a minimum of 1,000 cells from three to seven different isolations were analyzed.

DNA fragmentation analysis by gel electrophoresis. The RINm5F DNA fragmentation was assayed by agarose gel electrophoresis with ethidium bromide staining. After 3–6 h of incubation in medium containing or lacking 6 μmol/l staurosporine, cells (1×10^6) were centrifuged and resuspended in 250 μl of buffer containing 10 mmol/l Tris-HCl and 1 mmol/l EDTA with pH 8.0 (TE buffer). A lysis buffer (250 μl) containing 100 mmol/l Tris-HCl, 250 mmol/l NaCl, 5 mmol/l EDTA, and 0.2% SDS was added for 30 min at 4°C. Soluble DNA was separated from chromatin-bound DNA by centrifugation at 12,000*g* for 15 min. The pellet was discarded. For precipitating nucleic acids, 1 ml of ice-cold 99% ethanol and 30 μl of 5 mol/l NaCl was added to the supernatant for 1 h. The sample was centrifuged at 12,000*g* for 15 min at 4°C, and the pellet was dissolved in 30 μl of TE buffer. Four microliters of RNAse (0.5 mg/ml) was added, and the sample was incubated at 37°C for 1 h. Four microliters of Proteinase K (16 mg/ml) was added, and the sample was incubated at 37°C for 1 h. Loading buffer (8 μl) containing 40% glycerol, 0.35 mol/l Tris-HCl, 0.35 mol/l boric acid, 0.8 mmol/l EDTA, and 0.1% SDS with pH 8.3 was added, and the sample was stored overnight at 4°C. DNA fragments were separated on 1.8% agarose gel in a buffer containing 0.44 mol/l Tris-HCl, 0.44 mol/l boric acid, and 1 mmol/l EDTA with pH 8.3 in the presence of 0.5 mg/ml ethidium bromide, visualized under ultraviolet light, and photographed.

Measurements of activity of caspase-3–like proteases. RINm5F cells grown until 80% confluence were incubated with or without 6 μmol/l staurosporine in the presence or in the absence of 50 μmol/l Z-DEVD-fmk for 3 h. After incubation, cells were mechanically detached and washed twice in PBS and the activity of caspase-3–like proteases was measured using Apo Alert Caspase 3 assay kit (Clontech, Palo Alto, CA), according to the manufacturer's instructions.

Plasmids. The plasmid pFRET-KEAF was generated from yellow cameleon-2 (15) (provided by Dr. R.Y. Tsien, Department of Pharmacology, University of California San Diego, La Jolla, CA). The EYFP part was modified by site-directed mutagenesis, i.e., exchanging Val^{68} by Leu and Gln^{69} by Lys as described previously (16,17), thus obtaining a more pH-stable version of EYFP. The sequences coding for ECFP and $EYFP^{V68L,Q69K}$ were spaced by 72 nucleotides, encoding the 24–amino acid string RMHDQLTEEQIAEF*KEAF*SLFDKL. To obtain pFRET-DEVD, we mutated the nucleotides encoding the KEAF-sequence to code for DEVD within the spacer, e.g., RMHDQLTEEQIAEF*DEVD*SLFDKL. Site-directed mutagenesis was performed using the QuikChange Mutagenesis Kit (Stratagene, La Jolla, CA) and respective oligonucleotides, purchased from Genset (Paris, France). In pFRET2-DEVD, the expression cassette of the fusion gene was identical to that in pFRET-DEVD with the exception that the $EYFP^{V68L,Q69K}$ moiety was exchanged by the YFP-version Venus (18), which was provided by Dr. A. Miyawaki (Brain Science Institute, RIKEN, Saitama, Japan). The expression of the fusion gene was driven by the rat insulin-2 promoter fragment (−695/+1). Plasmids pEYFP and pECFP were generated by exchanging the cDNA of EGFP in pRcCMVi.EGFP (19) versus the cDNAs of $EYFP^{V68L,Q69K}$ and ECFP, respectively. All vector constructions were verified by DNA sequence analysis.

Cell transfection with plasmid constructs. RINm5F cells (passages 40–60) or MIN6 cells (passages 40–43) attached to coverslips were transiently transfected with pFRET-KEAF, pFRET-DEVD, pFRET2-DEVD, pECFP, or pEYFP using Lipofectamine 2000, according to the manufacturer's instructions. Cells that were transfected with pFRET-KEAF, pFRET-DEVD, or pFRET2-DEVD express fusion proteins abbreviated as C-KEAF-Y, C-DEVD-Y, or C-DEVD-Y2, respectively. Experiments with cells expressing the actual fusion proteins were performed within 48–72 h subsequent to transfection. For generation of stable RINm5F cell lines expressing C-DEVD-Y2, driven by the rat insulin-1 promoter fragment (−410/+1), transiently transfected cells were subcultured in 98-well plates that contained 350 μg/ml G418. After 10 days, G418-resistant colonies were subcloned in six-well plates grown to 75% confluence and assessed for FRET signal.

Microfluorometry for on-line single-cell detection of FRET. The coverslip with cells was mounted as the bottom of an open perfusion chamber that was used in an inverted microscope (Zeiss Axiovert 135TV; Carl Zeiss) connected to a SPEX fluorolog-2 system (Spex industries, Edison, NJ). Cells were maintained at 37°C by temperature-controlled metal jackets both on the perfusion chamber and on the 40×/1.3 oil immersion objective. Perfusion medium was RPMI 1640. The excitation was set to 440 nm, and fluorescence emission was split into two PMT (photomultiplier) detectors with bandpass filters 480 ± 15 nm (ECFP emission) and 535 ± 13 nm (EYFP emission) for simultaneous detection of the two channels.

TPLSM for on-line detection of FRET. The experiments with TPLSM were performed in a similar way as for microfluorometry (see above) with the perifusion chamber mounted on a Leica DMIRB microscope with a Leica TCS-NT confocal laser scanner (Leica Microsystems Heidelberg). We used a Ti:Sapphire laser (Tsunami; Spectra-Physics, Mountain View, CA) for ~100 fs excitation at ~82 MHz and two external PMT detectors (Hamamatsu R268; Hamamatsu Photonics, Shizuoka-Ken, Japan) with bandpass filters 480 ± 15 nm (ECFP emission) and 535 ± 13 nm (EYFP emission), arranged in-house for nondescanned fluorescence detection (20). The lens was Leica PL APO 100×/1.40 oil, and average excitation power was below 10 mW at 790 nm. Transmitted light with differential interference contrast (DIC) was detected simultaneously as the fluorescence detection. For detecting both FRET and chromatin condensation, stable RINm5F cells expressing C-DEVD-Y2 were loaded with Hoechst 33342 (1 μg/ml) for 5 min before the experiment, where the excitation wavelength was 820 nm.

Denoising procedure of TPLSM images. For reducing the level of random noise present in the raw fluorescence acquisition, the wavelet denoising technique was applied to the images before further processing. This technique allows one to achieve a space-adaptive smoothing of the images at low computational price, which makes it particularly suited for applications with two-photon microscopy. It has also proved to be very effective for confocal microscopy (21). In short, the method involves thresholding the images in wavelet space. A discrete wavelet transform (DWT) is first applied to the image. This produces a series of approximations of the original image at different scales. The original image can be recovered by applying an inverse DWT (22). The finest scales of the DWT are then thresholded by setting all wavelet coefficients whose magnitudes fall below a certain level to zero. After thresholding, the inverse DWT is applied and the denoised image is obtained. The relevant threshold level to be used must be estimated at each scale, which can be done by a mean-square analysis of the data. The specific thresholding procedure and DWT that were used are the ones described previously (21).

Quantification and visualization of FRET. The following ratio is often used as a measure of FRET between the donor (ECFP) and the acceptor (EYFP):

$$\mathrm{FRET} = \frac{\mathrm{Ff}}{\mathrm{Df}} \left(= \frac{\mathrm{EYFP}}{\mathrm{ECFP}} \right)$$

where "Ff" denotes the signal using the filters for acceptor emission when exciting the donor and "Df" denotes the signal using the filters for the donor emission when exciting the donor (using variable names from 23). The Ff/Df ratio was used as a measure of FRET in our microfluorometry experiments (Fig. 2). However, a significant "cross talk" as a result of fluorescence spectral overlap motivates correction, which is particularly important for quantitative FRET imaging. When exciting the donor (ECFP) in the absence of the acceptor (EYFP), the emission is detected not only using the filters for donor emission ("Dd") but also using the filters for acceptor emission ("Fd"). In our case, when using TPLSM, the ratio "Fd/Dd" was determined to be 0.32. When exciting at the donor excitation wavelength in the absence of donor (in the

presence of acceptor only), the emission from the acceptor ("Fa") was hardly detectable, meaning that we can exclude that type of cross talk correction. In agreement with equation 18 in (23), we then used

$$\mathrm{FRET}_{\mathrm{corr}} = \frac{\mathrm{Ffa}}{\mathrm{Dfd}} = \frac{\mathrm{Ff} - (\mathrm{Fd}/\mathrm{Dd})\,\mathrm{Df}}{\mathrm{Df}} \left(= \frac{\mathrm{EYFP}_{\mathrm{corr}}}{\mathrm{ECFP}}\right)$$

for our images (Figs. 3 and 5). For image processing, we used Matlab (The MathWorks, Natick, MA), and for visualization of three-dimensional data (Fig. 5), we used Imaris 2.4 (Bitplane, Zürich, Switzerland).

RESULTS

Caspase-3–like protease activity as an indicator of pancreatic β-cell apoptosis. For examining whether caspase-3–like enzymes mediate pancreatic β-cell apoptosis, mice β-cells were preincubated with a cell-permeable inhibitor of caspase-3–like proteases, Z-DEVD-fmk. Apoptosis was induced by incubation of cells in 17 mmol/l glucose or IL-1β for 40 h. The data obtained (Fig. 1*A* and *B*) demonstrate that Z-DEVD-fmk inhibited both high-glucose– and cytokine-induced apoptosis. This shows that a pathway mediated by caspase-3–like proteases is involved in β-cell apoptosis under both hyperglycemic and inflammatory conditions and suggests that monitoring of caspase-3–like activity can constitute the basis for on-line monitoring of apoptosis in living β-cells. For further development of the method, the β-cell line RINm5F was used. For shortening the time for on-line experiments, staurosporine was used as a well-known stimulator of apoptosis (24). Figure 1*C* shows that incubation of RINm5F cells with 6 μmol/l staurosporine for only 3 h gave rise to a DNA laddering pattern typical for apoptosis. This apoptotic change was preceded by activation of caspase-3–like proteases and could be inhibited by Z-DEVD-fmk (Fig. 1*D*).

On-line monitoring of apoptosis in insulin-secreting cells. For on-line detection of apoptosis using the FRET technique, RINm5F cells were transiently transfected with plasmids pFRET-KEAF or pFRET-DEVD. Single cells were monitored as described above using microfluorometry (Fig. 2*A* and *B*). The data obtained demonstrated that activation of caspase-3–like proteases by staurosporine in cells transfected with pFRET-DEVD and expressing the fusion protein C-DEVD-Y lead to loss of FRET within 155 ± 23 min (mean ± SE; $n = 9$; Fig. 2*A*). On the contrary, cells transfected with pFRET-KEAF and expressing a fusion protein possessing the amino acid sequence KEAF (C-KEAF-Y) instead of the specific sequence for caspase-3–like proteases DEVD did not show loss of FRET in the presence of 6 μmol/l staurosporine during the time of experiment (at least up to 330 min) or before the cell detached (out of reach for detection; Fig. 2*B*). Hence, one can conclude that the loss of FRET observed in Fig. 2*A* is specific to the cleavage of C-DEVD-Y and thus reflected activation of caspase-3–like proteases. Longer incubation of cells with staurosporine finally led to a decrease in fluorescence to the background level (data not shown). This effect could be explained by the disappearance of cells from the focus of the microscope. In recordings performed the same way but using MIN6 cells expressing

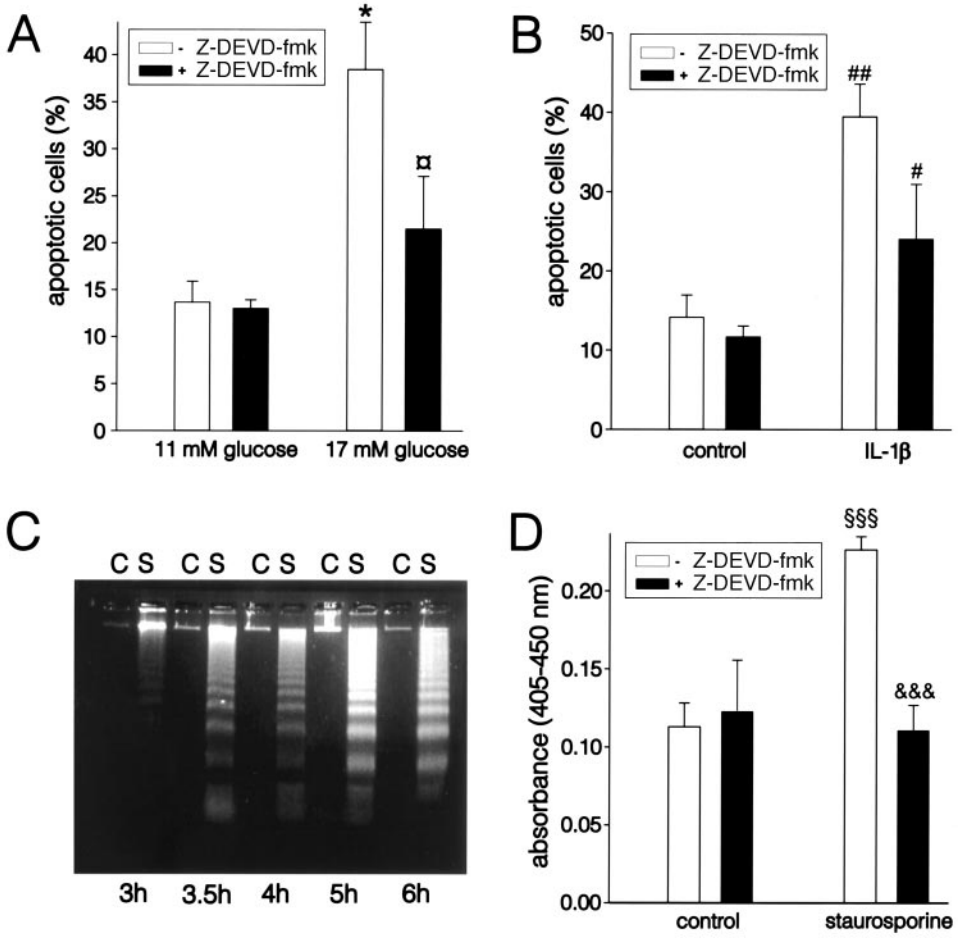

FIG. 1. Effect of inhibitor of caspase-3–like proteases (Z-DEVD-fmk, 50 μmol/l) on apoptosis induced by 17 mmol/l glucose (*A*) or 2 ng/ml IL-1β (*B*) in *ob/ob* mouse pancreatic β-cells. Data are expressed as means ± SE (P* < 0.05 vs. 11 mmol/l glucose; ¤*P* < 0.05 vs. 17 mmol/l glucose; ##*P* < 0.01 vs. control; #*P* < 0.05 vs. IL-1β; *n* = 3). Staurosporine activates apoptosis and caspase-3–like proteases in insulin-producing RIN5mF cells (*C* and *D*). *C*: DNA fragmentation in control (C) and staurosporine-treated (S; 6 μmol/l) RIN5mF cells after different times of treatment (*n* = 3) *D*: Effect of Z-DEVD-fmk (10 μmol/l) on staurosporine-induced (6 μmol/l) caspase-3 activity in RINm5F cells after 3 h of incubation. Enzyme activity was measured in cell lysates by spectrophotometric detection using caspase-3 substrate DEVD-*p*-nitroaniline. Data are expressed as means ± SE (§§§*P* < 0.001 vs. control; &&&*P* < 0.001 vs. staurosporine; *n* = 4 without Z-DEVD-fmk; *n* = 3 with Z-DEVD-fmk).**

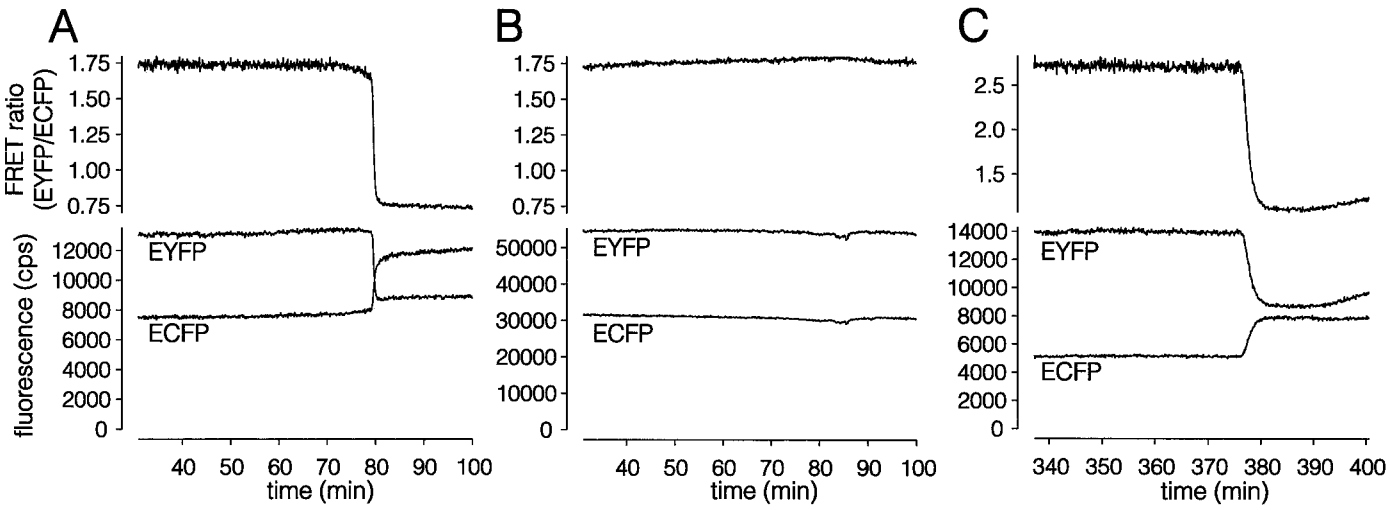

FIG. 2. Microfluorometric on-line detection of cells expressing FRET proteins in response to 6 μmol/l staurosporine (given from time 0). *A*: RINm5F cell expressing C-DEVD-Y (representative of $n = 9$). *B*: RINm5F cell expressing C-KEAF-Y (representative of $n = 5$). *C*: MIN6 cell expressing C-DEVD-Y2 (representative of $n = 4$).

the modified construct C-DEVD-Y2 (Fig. 2*C*), the FRET loss appeared later (257 ± 59 min, $n = 4$) than in the above experiments, although this was not significantly later according to *t* test. As expected, C-DEVD-Y2 gave a stronger EYFP signal relative to the ECFP signal compared with C-DEVD-Y. Because the expression of C-DEVD-Y2 was driven by the rat insulin-2 promoter fragment, we here demonstrate a vector that selectively expresses C-DEVD-Y2 in insulin-expressing cells.

To look more in detail into the cellular events underlying apoptosis, we used TPLSM. Figure 3 shows one focal plane of two C-DEVD-Y–expressing cells undergoing apoptosis in response to 6 μmol/l staurosporine, and the corresponding DIC images illustrate the cell shape. C-DEVD-Y was distributed in the cytoplasm (Fig. 3), and this distribution and fluorescence amplitude were stable for a long time in cells in the absence of apoptotic stimulator (data not shown). Activation of caspase-3–like proteases took place in the presence of 6 μmol/l staurosporine. This, at first, led to a decrease in EYFP fluorescence emission and an increase in ECFP fluorescence emission in the cytoplasm when exciting ECFP, both of which implicated a loss of FRET (Fig. 3). Thereafter, fluorescence corresponding specifically to ECFP emission appeared in the nucleus. The last event occurred very quickly (<1 min). On the contrary, no changes were observed in cells expressing C-KEAF-Y during the same period of time (data not shown). It is interesting that C-KEAF-Y was distributed

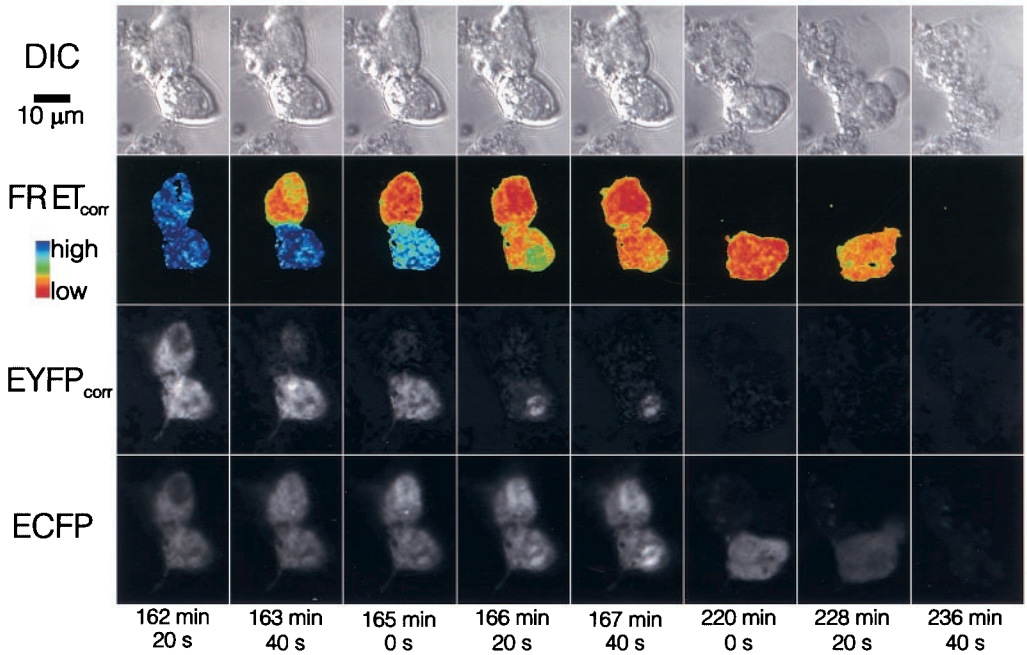

FIG. 3. TPLSM on-line imaging of one focal plane showing two C-DEVD-Y–expressing RINm5F cells at the time points indicated. DIC shows the cell morphology. FRET$_{corr}$ shows the corrected FRET images (see RESEARCH DESIGN AND METHODS) with a color scale as shown, with blue indicating high level and red indicating low level of FRET$_{corr}$. EYFP$_{corr}$ is the EYFP signal corrected for spectral overlap from ECFP emission. Staurosporine (6 μmol/l) was given from time 0 ($n = 3$ experiments with a total of eight cells).

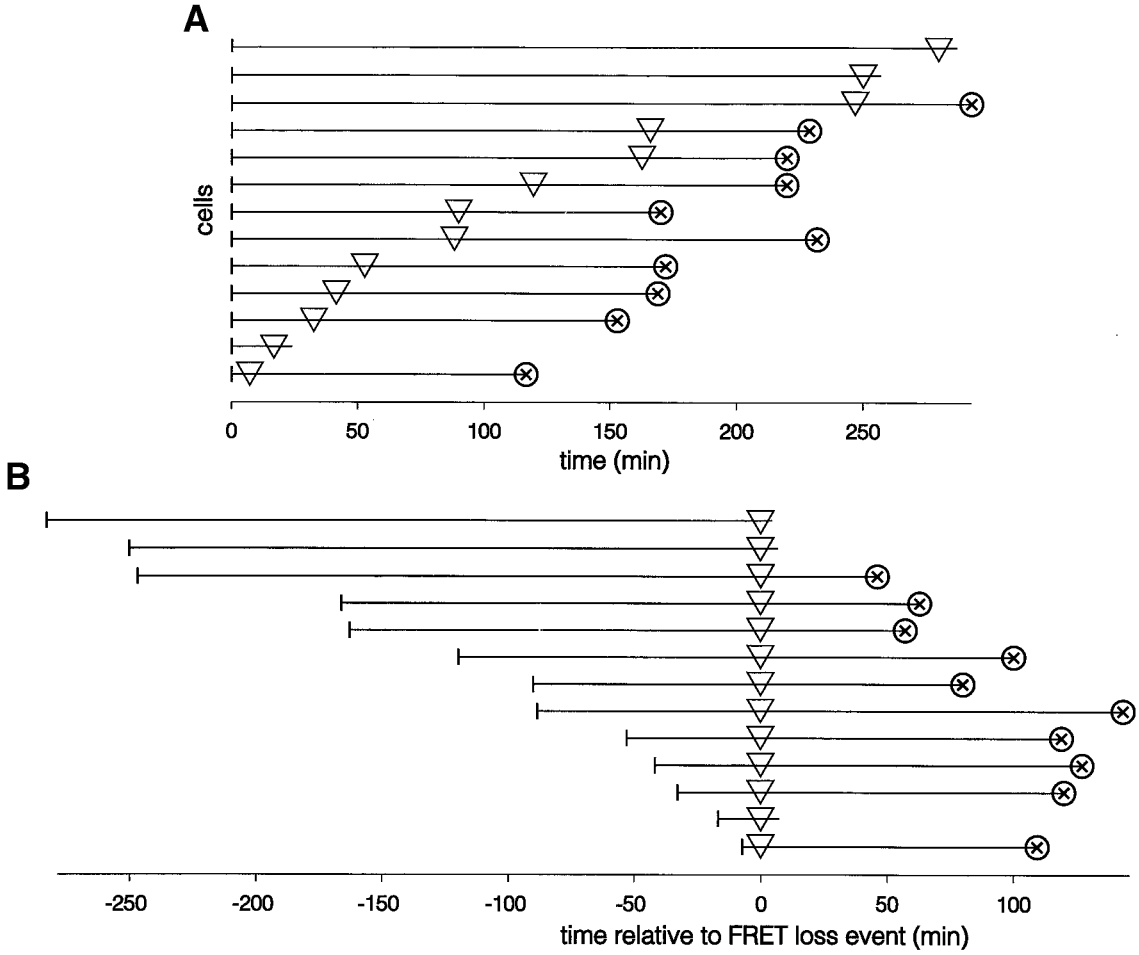

FIG. 4. Visualization of the times for FRET loss (▽) and cell loss/detachment (⊗) in 13 cells in experiments similar to the one in Fig. 3. Each line indicates one cell, and the start of the experiment (start of addition of 6 μmol/l staurosporine) is indicated by a vertical line. *A*: Data relative to the start of the experiment. *B*: Same data relative to the time for FRET loss. Cells are sorted according to the time from start to FRET loss.

not only in the cytosol but also in the nucleus. For characterizing the cellular distribution of ECFP and EYFP, the breakdown products of caspase-3–mediated C-DEVD-Y proteolysis, RINm5F cells were transfected with constructs expressing ECFP and EYFP, respectively. These fluorescent proteins were distributed both in the cytoplasm and in the nucleus (data not shown), and the obtained images were used to calculate the fluorescence cross-talk correction factor "Fd/Dd" (see RESEARCH DESIGN AND METHODS). Loss of FRET in these experiments occurred after 120 ± 26 min (n = 13), and ECFP fluorescence disappeared after an additional 97 ± 11 min (n = 10; Fig. 4). Loss of ECFP fluorescence corresponded to rupture and disappearance of the cell as shown in the DIC images in Fig. 3.

Further spatial and temporal information can be obtained from scanning a stack of focal planes in a time-lapse mode, giving four-dimensional data (three spatial dimensions plus time). Figure 5 shows a four-dimensional series with three-dimensional reconstructed $FRET_{corr}$ data, when scanning 40 sections every 10 min, and demonstrates that subsequent to activation of caspase-3 and FRET disappearance, the cell started to round up and detach.

For confirming that the changes in FRET reflected apoptosis, stable RINm5F cells expressing C-DEVD-Y2 were loaded with the DNA staining dye Hoechst 33342 to allow simultaneous detection of both FRET disappearance and chromatin condensation, a characteristic feature of apoptosis, in cells treated with staurosporine. Figure 6 shows one cell before (237 min) and after (252 min) FRET disappearance and after pronounced chromatin condensation in the nucleus (267 min). Notably, the chromatin condensation can be observed both with Hoechst 33342 fluorescence and with DIC.

DISCUSSION

During the past few years, several key mediators of the induction and execution reaction cascades in cells undergoing apoptosis have been identified as a family of aspartic acid–specific cysteine proteases, the caspases (1,25). These enzymes exist in the cell as inactive proenzymes that are proteolytically processed and activated when the cell is undergoing apoptosis. Among caspases, caspase-3–like proteases, which recognize and cleave the DEVD sequence in their substrates, have been implicated as major mediators of the death signal in different types of cells (1). In this study, using an inhibitor of caspase-3–like proteases, Z-DEVD-fmk, we have shown that activation of these enzymes also takes place in high-glucose– and cytokine-induced apoptosis in pancreatic β-cells. This gives us the opportunity to use activation of caspase-3–like

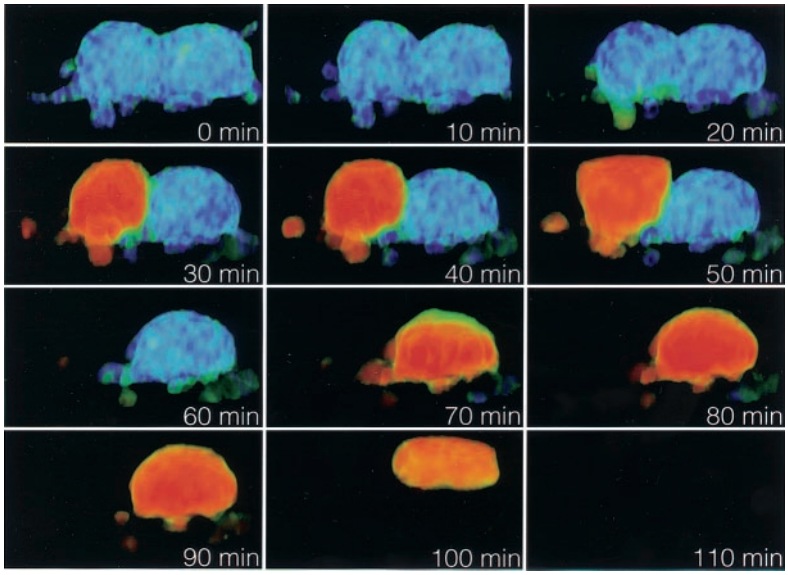

FIG. 5. TPLSM imaging in four dimensions (three-dimensional plus time) of $FRET_{corr}$ in two C-DEVD-Y–expressing RINm5F cells at the time points indicated. Staurosporine (6 μmol/l) was given from time 0. Every image is a three-dimensional volume rendered projection seen from the side of the cells, and the color scale is the same as used for $FRET_{corr}$ in Fig. 3 (n = 6 cells in two experiments).

proteases as a marker for pancreatic β-cell apoptosis. We have chosen fluorescence detection as a noninvasive method for on-line monitoring of apoptosis in living cells. In particular, the FRET technique based on the expression of a hybrid protein consisting of the two fluorescent proteins ECFP and EYFP, linked by a spacer containing the sequence DEVD, has been used. The feasibility of using similar hybrid proteins for end-point detection of apoptosis in Cos-7 cells (7,26), HeLa cells (27), 293 cells (28), and Rat-1/c-myc^{ER} fibroblasts (26) has been described. Similar proteins have recently been used for on-line detection of caspase-3 activation in Cos-7 cells (24), HeLa cells (29,30), and SHEP cells (30). Our results in this study clearly demonstrate that this technique can be used for on-line monitoring of apoptosis in living insulin-secreting cells.

We used staurosporine-induced apoptosis in RINm5F cells as a model system for development of the FRET technique for on-line detection of β-cell apoptosis. Both DNA laddering data and investigation of cell morphology showed that staurosporine at a concentration of 6 μmol/l induced β-cell apoptosis in RINm5F cells within 2–4 h. This process was mediated by caspase-3–like proteases as it was blocked in the presence of the inhibitor of these enzymes. Moreover, the pFRET-KEAF–transfected cells expressing the fusion protein C-KEAF-Y, lacking the DEVD sequence, did not show loss of FRET.

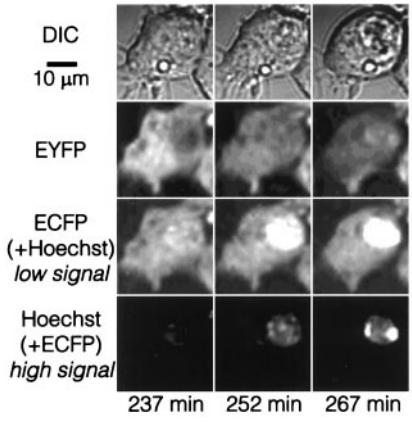

FIG. 6. TPLSM imaging of both FRET loss and subsequent chromatin condensation in stable RINm5F cells expressing C-DEVD-Y2 loaded with the DNA staining dye Hoechst 33342. DIC shows cell morphology. Most Hoechst 33342 fluorescence displays in the ECFP channel, where the high-amplitude nuclear signal can be considered as Hoechst 33342 fluorescence and the low-amplitude cytoplasmic signal can be considered as ECFP fluorescence. Staurosporine (6 μmol/l) was given from time 0. The EYFP signal was not corrected for spectral overlap, explaining the incomplete loss of signal after disappearance of FRET (n = 3 experiments with a total of at least nine cells).

The obtained data are in line with the involvement of caspase-3–like proteases in staurosporine-induced apoptosis shown previously in the SV40-transformed human fibroblast cell line GM701 (31). Our experiments with pFRET2-DEVD demonstrated that a vector selectively expressed in insulin-producing cells can be used for monitoring apoptosis of β-cells in a mixed cell population consisting of insulin- and non–insulin-producing cells. The pancreatic islet clearly represents such a mixed cell population.

FRET is widely used to study dynamics of the proximity between two fluorophores (32). In particular, the use of fluorescent proteins within genetically engineered FRET probes allows real-time monitoring of various cellular events. The FRET pair with ECFP as donor and EYFP as acceptor is now often used even if one problem with this particular FRET pair is the high degree of spectral overlap, with ECFP emission bleeding over to the EYFP detection channel (33). We therefore believe that careful corrections such as the one applied in this study are necessary to obtain useful quantitative data (23), especially in FRET imaging studies. Here we used a normal microfluorometric technique, based on epifluorescence microscopy, as well as TPLSM based on two-photon excitation. Both techniques use one wavelength for exciting the donor (ECFP) and two wavelengths for detecting emission from donor (ECFP) and acceptor (EYFP), respectively. The difference lies in excitation wavelength, light source, and instrument setup. TPLSM allows confocal images that can be obtained deeper in a tissue when compared with a normal confocal laser-scanning microscope (9,10). This in combination with focally limited photo damage makes TPLSM useful for studies of cells in vivo (34). We conclude in this study that TPLSM can be used to study FRET and induction of apoptosis using the C-DEVD-Y construct in insulin-producing cells. The ECFP-EYFP FRET pair was previously used

with TPLSM to monitor cytoplasmic free Ca^{2+} concentration (16). One important consideration in studies of living cells in general and apoptosis in particular is the degree of photo damage generated by the excitation light. We therefore performed separate control experiments monitoring cells not exposed to the apoptotic inducer staurosporine, and these cells were clearly viable for a longer time. The TPLSM technique gave a relatively low signal and consequently a high noise level, as a result of the limitation of photons. Therefore, we applied a three-dimensional filtering technique based on wavelets for denoising our image series. This kind of filtering preserves the quantitative, spatial, and temporal information to a high degree and is therefore appropriate to use for the data presented.

Monitoring of apoptosis on-line using TPLSM allowed us to analyze not only the loss of FRET but also the subcellular localization of the fluorescent proteins. At the beginning, all C-DEVD-Y fluorescence was distributed in the cytoplasm. Subsequent to induction of apoptosis, i.e., activation of caspase-3–like activity, and notion of loss of FRET of C-DEVD-Y in cytoplasm, ECFP fluorescence quickly appeared in the nucleus. Appearance of fluorescence in the nucleus in pFRET-DEVD–transfected cells can have at least two explanations. First, appearance of ECFP fluorescence can be explained by the disturbance in the nuclear envelope during apoptosis (35), making the translocation of C-DEVD-Y to the nucleus feasible. As caspase-3–like proteases are distributed to a large extent in the nucleus upon activation, they will cleave C-DEVD-Y, resulting in ECFP fluorescence. Second, appearance of ECFP fluorescence in the nucleus can be explained by diffusion of ECFP through nuclear pores subsequent to the breakage of C-DEVD-Y. To discriminate between these two alternatives, experiments have been performed with cells expressing ECFP or EYFP, after transfection with either pECFP or pEYFP (data not shown). The data obtained clearly show that both proteins enter the nucleus. This favors the conclusion that it is a breakdown product of C-DEVD-Y that goes from the cytoplasm to the nucleus. Moreover, we have not been able to see FRET in the nucleus in the cells in which C-DEVD-Y was expressed. In contrast, the fusion protein C-KEAF-Y, expressed in pFRET-KEAF–transfected cells, was distributed both in the cytoplasm and in the nucleus. Activation of caspase-3–like proteases neither changed this distribution nor broke C-KEAF-Y.

In the on-line studies performed, we were able to estimate the time sequence of events in staurosporine-induced apoptosis of RINm5F cells. According to our results, staurosporine induced activation of caspase-3–like proteases (loss of FRET) in ~90–180 min in RINm5F cells with a great variability. Approximately 90–110 min after the FRET loss, the cells rounded up and detached from the substrate or ruptured. The round-up of cells can be explained by breakage of cytoskeleton by the activated enzymes (36). The relatively constant time between FRET loss and disappearance of cells suggests that once the caspases are activated, the subsequent reactions of apoptosis are programmed in time. Full statistical characterization of this highly variable time sequence would require a significantly larger group of single-cell data. This would be possible to achieve with the actual technique, but the microscope setup should then be modified and adapted for collection of data from multiple cells.

We have now been able for the first time to *1*) monitor the time for activation of caspase-3–like proteases in single insulin-secreting cells and the subsequent detachment from the surface to which they adhere and *2*) monitor the activation of the caspase-3–like proteases in three dimensions using TPLSM. An important issue to consider is also that the technique used is not dependent on loading of substrate fluorescent dyes (37), because the FRET-DEVD technique is based on the expression of a fluorescent protein. The possibility to express fluorescent proteins in targeted tissues of transgenic mice will give a real opportunity to monitor apoptosis in cells and tissues in vivo, especially in combination with the TPLSM technique.

ACKNOWLEDGMENTS

This work was supported by grants from the Karolinska Institutet, the Novo Nordisk Foundation, the National Institutes of Health (DK-58508), the Swedish Research Council, the Swedish Diabetes Association, the Juvenile Diabetes Research Foundation International, AFA Sickness Insurance, and Berth von Kantzow's Foundation.

REFERENCES

1. Pick A, Clark J, Kubstrup C, Levisetti M, Pugh W, Bonner-Weir S, Polonsky KS: Role of apoptosis in failure of β-cell mass compensation for insulin resistance and β-cell defects in the male Zucker diabetic fatty rat. *Diabetes* 47:358–364, 1998
2. Mauricio D, Mandrup-Poulsen T: Apoptosis and the pathogenesis of IDDM: a question of life and death. *Diabetes* 47:1537–1543, 1998
3. Juntti-Berggren L, Larsson O, Rorsman P, Ämmälä C, Bokvist K, Wåhlander K, Nicotera P, Dypbukt J, Orrenius S, Hallberg A, Berggren PO: Increased activity of L-type Ca^{2+} channels exposed to serum from patients with type I diabetes. *Science* 261:86–90, 1993
4. Lorenzo A, Razzaboni B, Weir GC, Yankner BA: Pancreatic islet cell toxicity of amylin associated with type-2 diabetes mellitus. *Nature* 368: 756–760, 1994
5. Koyama M, Wada R, Sakuraba H, Mizukami H, Yagihashi S: Accelerated loss of islet beta cells in sucrose-fed Goto-Kakizaki rats, a genetic model of non-insulin-dependent diabetes mellitus. *Am J Pathol* 153:537–545, 1998
6. Efanova IB, Zaitsev SV, Zhivotovsky B, Köhler M, Efendic S, Orrenius S, Berggren PO: Glucose and tolbutamide induce apoptosis in pancreatic beta-cells. A process dependent on intracellular Ca^{2+} concentration. *J Biol Chem* 273:33501–33507, 1998
7. Mahajan NP, Harrison-Shostak DC, Michaux J, Herman B: Novel mutant green fluorescent protein protease substrates reveal the activation of specific caspases during apoptosis. *Chem Biol* 6:401–409, 1999
8. Chiang CF, Okou DT, Griffin TB, Verret CR, Williams MN: Green fluorescent protein rendered susceptible to proteolysis: positions for protease-sensitive insertions. *Arch Biochem Biophys* 394:229–235, 2001
9. Denk W, Strickler JH, Webb WW: Two-photon laser scanning fluorescence microscopy. *Science* 248:73–76, 1990
10. Piston DW: Imaging living cells and tissues by two-photon excitation microscopy. *Trends Cell Biol* 9:66–69, 1999
11. Zaitsev SV, Köhler M, Loiko II, Leibiger B, Leibiger I, Appelskog I, Kapelioukh I, Berggren PO: Online monitoring of apoptosis in living pancreatic beta-cells (Abstract). *Diabetologia* 45 (Suppl. 2):A149, 2002
12. Nilsson T, Arkhammar P, Hallberg A, Hellman B, Berggren PO: Characterization of the inositol 1,4,5-trisphosphate-induced Ca2+ release in pancreatic beta-cells. *Biochem J* 248:329–336, 1987
13. Hellman B: Methodological approaches to studies on the pancreatic islets. *Diabetologia* 6:110–120, 1970
14. Lernmark Å: The preparation of, and studies on, free cell suspensions from mouse pancreatic islets. *Diabetologia* 10:431–438, 1974
15. Miyawaki A, Llopis J, Heim R, McCaffery JM, Adams JA, Ikura M, Tsien RY: Fluorescent indicators for Ca^{2+} based on green fluorescent proteins and calmodulin. *Nature* 388:882–887, 1997
16. Fan GY, Fujisaki H, Miyawaki A, Tsay RK, Tsien RY, Ellisman MH:

Video-rate scanning two-photon excitation fluorescence microscopy and ratio imaging with cameleons. *Biophys J* 76:2412–2420, 1999
17. Miyawaki A, Griesbeck O, Heim R, Tsien RY: Dynamic and quantitative Ca^{2+} measurements using improved cameleons. *Proc Natl Acad Sci U S A* 96:2135–2140, 1999
18. Nagai T, Ibata K, Park ES, Kubota M, Mikoshiba K, Miyawaki A: A variant of yellow fluorescent protein with fast and efficient maturation for cell-biological applications. *Nat Biotechnol* 20:87–90, 2002
19. Moede T, Leibiger B, Pour HG, Berggren PO, Leibiger IB: Identification of a nuclear localization signal, RRMKWKK, in the homeodomain transcription factor PDX-1. *FEBS Lett* 461:229–234, 1999
20. Piston DW, Bennett BD, Ying G: Imaging of cellular dynamics by two-photon excitation microscopy. *Microsc Microanal* 1:25–34, 1995
21. Boutet de Monvel J, Le Calvez S, Ulfendahl M: Image restoration for confocal microscopy: improving the limits of deconvolution, with application to the visualization of the mammalian hearing organ. *Biophys J* 80:2455–2470, 2001
22. Mallat S: *A Wavelet Tour of Signal Processing*. San Diego, CA, Academic Press New York, 1999
23. Gordon GW, Berry G, Liang XH, Levine B, Herman B: Quantitative fluorescence resonance energy transfer measurements using fluorescence microscopy. *Biophys J* 74:2702–2713, 1998
24. Tyas L, Brophy VA, Pope A, Rivett AJ, Tavare JM: Rapid caspase-3 activation during apoptosis revealed using fluorescence-resonance energy transfer. *EMBO Rep* 1:266–270, 2000
25. Nunez G, Benedict MA, Hu Y, Inohara N: Caspases: the proteases of the apoptotic pathway. *Oncogene* 17:3237–3245, 1998
26. Harpur AG, Wouters FS, Bastiaens PI: Imaging FRET between spectrally similar GFP molecules in single cells. *Nat Biotechnol* 19:167–169, 2001
27. Tawa P, Tam J, Cassady R, Nicholson DW, Xanthoudakis S: Quantitative analysis of fluorescent caspase substrate cleavage in intact cells and identification of novel inhibitors of apoptosis. *Cell Death Differ* 8:30–37, 2001
28. Xu X, Gerard AL, Huang BC, Anderson DC, Payan DG, Luo Y: Detection of programmed cell death using fluorescence energy transfer. *Nucleic Acids Res* 26:2034–2035, 1998
29. Luo KQ, Yu VC, Pu Y, Chang DC: Application of the fluorescence resonance energy transfer method for studying the dynamics of caspase-3 activation during UV-induced apoptosis in living HeLa cells. *Biochem Biophys Res Commun* 283:1054–1060, 2001
30. Morgan MJ, Thorburn A: Measurement of caspase activity in individual cells reveals differences in the kinetics of caspase activation between cells. *Cell Death Differ* 8:38–43, 2001
31. Jacobsen MD, Weil M, Raff MC: Role of Ced-3/ICE-family proteases in staurosporine-induced programmed cell death. *J Cell Biol* 133:1041–1051, 1996
32. Clegg RM: Fluorescence resonance energy transfer. *Curr Opin Biotechnol* 6:103–110, 1995
33. Pollok BA, Heim R: Using GFP in FRET-based applications. *Trends Cell Biol* 9:57–60, 1999
34. Helmchen F, Denk W: New developments in multiphoton microscopy. *Curr Opin Neurobiol* 12:593, 2002
35. Faleiro L, Lazebnik Y: Caspases disrupt the nuclear-cytoplasmic barrier. *J Cell Biol* 151:951–959, 2000
36. Wolf BB, Green DR: Suicidal tendencies: apoptotic cell death by caspase family proteinases. *J Biol Chem* 274:20049–20052, 1999
37. Komoriya A, Packard BZ, Brown MJ, Wu ML, Henkart PA: Assessment of caspase activities in intact apoptotic thymocytes using cell-permeable fluorogenic caspase substrates. *J Exp Med* 191:1819–1828, 2000